Elastic properties of Sierpinski-like carpets: Finite-element-based simulation

V. G. Oshmyan,[1] S. A. Patlazhan,[2] and S. A. Timan[1]
[1]*N. N. Semenov Institute of Chemical Physics, Russian Academy of Sciences, 4 Kosygin Street, Moscow 119991, Russia*
[2]*Institute of Problems of Chemical Physics, Russian Academy of Sciences, Chernogolovka, Moscow Region 142432, Russia*
(Received 4 April 2000; revised manuscript received 18 June 2001; published 19 October 2001)

The elastic properties of two-dimensional continuous composites of fractal structures are studied with the set of Sierpinski-like carpets filled by voids or rigid inclusions. The effective elastic moduli of these carpets are calculated numerically using the finite-element and position-space renormalization group techniques. The fixed-point problem is analyzed by flow diagrams in the plane of the current Poisson ratios and coefficients of anisotropy of the composites. It is found that in the general case the effective elastic moduli asymptotically approach a power-law behavior. Moreover, the common exponent characterizes the scaling behavior of each component of the elastic modulus tensor of a definite carpet. The values of the scaling exponents and positions of the fixed points are shown to be independent of the elastic properties of the host and depend significantly on the fractal dimension of the composite.

DOI: 10.1103/PhysRevE.64.056108 PACS number(s): 05.50.+q

I. INTRODUCTION

Elastic properties of fractal structures have been intensively studied since 1984 [1–6]. Discrete spring-based models of isotropic percolation clusters or the triangular Sierpinski gasket have usually been considered. These structures are shown to be described by two independent effective elastic constants, say, the Lamé coefficients λ and μ, which just depend on the rigidity and the fraction of springs. If the size L of the system is less than the correlation length it was found that both λ and μ exhibit power-law (scaling) behavior $\lambda, \mu \propto L^{-\tau}$, with the *same* value of the exponent τ.

In contrast to the spring-based systems, composite materials are usually treated in the framework of continuum mechanics. Also, the structure of real matrix composites does not need to follow the percolation models: the aggregation of inclusions could bring a variety of morphologies characterized by different fractal dimensions [7]. In its turn, this could affect composite elastic properties. The first attempt at studying the effective elasticity of continuous fractal composites was made by Sheng and Tao [8] with the porous Sierpinski carpet (see Fig. 1). Due to the square symmetry of this model three independent components C_{1111}, C_{1122}, and C_{1212} of the effective elastic modulus tensor C_{ijkl} describe its elastic properties. They were calculated in the long-wave limit of the Dyson equation for elastic scattering waves. The surprising message of Ref. [8] was that the effective moduli C_{1111}, $C_{1111}-C_{1122}$, and C_{1212} exhibit different scaling behavior as functions of dimensionless size $L=l/a$ of the carpet. The values l and a are the sizes of the largest (outer) side of the carpet and the thinnest part of the host ligament between the inclusions (see Fig. 1). In the latter case a coincides with the size of the smallest inclusion. The corresponding exponents were estimated to equal $\tau_1 \approx 0.27$, $\tau_2 \approx 0.25$, and $\tau_3 \approx 0.46$. A close result was obtained by Patlazhan [9] in the framework of a different approach. Based on two simplifications (the square inclusions were replaced by circles of the same area and uniformity of the strains inside the inclusions was assumed) it was obtained that $\tau_1 \approx 0.25$, $\tau_2 \approx 0.26$, $\tau_3 \approx 0.33$ for the porous Sierpinski carpet. Additionally, the case of rigid inclusions was analyzed in Ref. [9]. This results in a scaling law $C_{ijkl} \propto L^{s_p}$ characterized by the other values of the exponents. It was found that they are equal to $s_1 \approx s_2 \approx s_3 \approx 0.14$ for the same moduli C_{1111}, $C_{1111}-C_{1122}$, and C_{1212}. This fact indicates that the scaling properties of elastic Sierpinski carpets filled by voids or rigid inclusions are different.

The results obtained in Refs. [8,9] for the continuous porous Sierpinski carpet are in qualitative contradiction with those obtained for lattice isotropic fractals. The main difference is that the axial and shear moduli of the porous carpet demonstrate *distinct* scaling behavior. In spite of the suggestion that this observation might be explained either as an inherent property of the anisotropic carpet or by breaking the analogy between the discrete and continuous elastic models [8], the nature of this discrepancy has remained unclear. It should be noted that these results were obtained just for the three initial generations (stages) of the Sierpinski carpet corresponding to $L=3$, 3^2, and 3^3 (see Fig. 1). A dipper partition of the fractal makes direct calculations of the effective moduli extremely cumbersome. Also, the exponents calculated in Refs. [8,9] were derived just for the single value of the host Poisson ratio $\nu^{(0)}=0.2$. These points provide at least two questions: (i) whether the same scaling behavior would be valid for the developed generations (large L) of the carpet and (ii) how the results would vary with change of the elastic characteristics of a host.

Apart from these questions another important problem arises: How do the scaling properties depend on the struc-

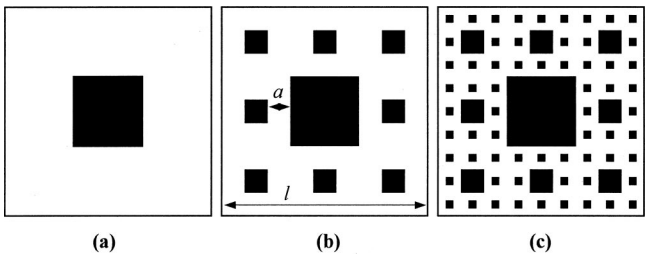

FIG. 1. Three initial generations of the classical Sierpinski carpet. (a) $n=1$, $L=3$; (b) $n=2$, $L=9$; (c) $n=3$, $L=27$.

ture, specifically on the fractal dimension, of the composite? Actually, for many reasons it is important to know the extent to which the elastic moduli are affected by the fractal dimension. In order to answer this problem, here we introduce a set of similar fractals of square symmetry characterized by other fractal dimensions (see Fig. 9 below). These structures can be called Sierpinski-like carpets. A common feature of the carpets is that they have the same symmetry and thus can be described by three independent effective elastic moduli. This makes it possible to find a correlation of the elastic properties of the composites with the fractal dimensions.

To estimate the scaling properties of the effective elastic moduli of the developed generations of the fractals the position-space renormalization group (PSRG) is considered in this paper. The main idea of this technique is that the effective elastic moduli, calculated for some generation, are used in the same stage of the carpet as renormalized moduli of the host. Then this procedure is reiterated. The effective moduli of each step are calculated numerically by means of the finite-element method (FEM). As long as the number of iterations is arbitrary, the effective elastic moduli of any generation of a carpet can be approximated in this way. To prove the scaling behavior of the effective elastic moduli at sufficiently large L, a fixed-point problem is studied in the plane of the current effective Poisson ratios $\nu = C_{1122}/C_{1111}$ and coefficients of anisotropy $\alpha = (C_{1111} - C_{1122})/(2C_{1212})$, in the framework of the suggested procedure.

This paper is organized as follows. The method of calculation of effective elastic moduli of fractal composites is described in the second section. It is divided into two subsections. The constitutive equations adapted to use the finite-element method for the classical Sierpinski carpet are represented in the first one. It provides a method of direct calculation of the effective elastic moduli for several initial generations of the fractal. In the second subsection the PSRG procedure to simulate elastic properties of the developed fractal structures is formulated. The results of this approach are discussed in the third section taking the classical Sierpinski carpet as an example. The scaling behavior of the effective moduli and the fixed-point problem are analyzed for carpets filled by voids and rigid particles. The elastic properties of Sierpinski-like carpets are studied in the fourth section. The dependence of the effective elastic properties of these structures on the fractal dimension is derived and discussed.

II. CALCULATION OF EFFECTIVE ELASTIC MODULI: GENERAL SCHEME

A. Finite-element model

For the sake of definiteness we begin with the classical Sierpinski carpet. Its first three stages are shown in Fig. 1. The white (host) and black (inclusions) areas of the fractal are supposed to exhibit different rigidities. They are described by the local elastic modulus tensor $c_{ijkl}(\mathbf{r})$, equal to $c_{ijkl}(\mathbf{r}) = c_{ijkl}^{\text{host}}$ if $\mathbf{r}$ belongs to the host or $c_{ijkl}(\mathbf{r}) = c_{ijkl}^{\text{inc}}$ otherwise. We will assume that the tensor of the elastic moduli of the host is congruent to the square symmetry of the carpet. Two main types of inclusion are considered in this work: voids ($c_{ijkl}^{\text{inc}} = 10^{-9} c_{ijkl}^{\text{host}}$ in the numerical simulations) and rigid particles ($c_{ijkl}^{\text{inc}} = 10^{9} c_{ijkl}^{\text{host}}$). In accordance with the terminology accepted in percolation problems and to shorten further exposition, the composites filled by voids and rigid inclusions will be called *elastic* and *superelastic carpets*, respectively.

The local displacements $\mathbf{u}(\mathbf{r})$ and the elastic moduli $c_{ijkl}(\mathbf{r})$ define the local strain and stress according to the definitions $\varepsilon_{kl}(\mathbf{r}) = [u_{k,l}(\mathbf{r}) + u_{l,k}(\mathbf{r})]/2$ and $\sigma_{ij}(\mathbf{r}) = c_{ijkl}(\mathbf{r})\varepsilon_{kl}(\mathbf{r})$. The effective elastic properties of the nth generation of the carpet, indicated as $\Omega^{(n)}$, are defined by the tensor of the effective moduli $C_{ijkl}^{(n)}$. It determines the relationship between the mean strain $\varepsilon_{ij}^{(n)}$ and the mean stress $\sigma_{ij}^{(n)}$ tensors of $\Omega^{(n)}$:

$$\sigma_{ij}^{(n)} = C_{ijkl}^{(n)} \varepsilon_{kl}^{(n)}. \tag{1}$$

We assume that $\varepsilon_{ij}^{(n)} = (1/\Omega^{(n)}) \int_{\Omega^{(n)}} \varepsilon_{ij}(\mathbf{r}) d^2 r$, as an example. In the case of the Sierpinski carpet the dimensionless size L of $\Omega^{(n)}$ is equal to $L = 3^n$. Therefore, it is natural to consider the uniform host as the zeroth generation $\Omega^{(0)}$ of the carpet and to set $C_{ijkl}^{(0)} = c_{ijkl}^{\text{host}}$. In order to obtain effective elastic moduli from Eq. (1) the spatial distribution of local displacements in the composite has to be calculated under definite boundary conditions. This can be studied in the framework of the variation principle for the elastic energy

$$w(\mathbf{u}) = \frac{1}{2} \int_{\Omega^{(n)}} [c_{1111}(u_{1,1}^2 + u_{2,2}^2) + 2c_{1122} u_{1,1} u_{2,2} + c_{1212}(u_{1,2} + u_{2,1})^2] dx_1 dx_2. \tag{2}$$

In the present paper this problem is numerically solved by using the FEM.

For this purpose a uniform square lattice is imposed on the carpet with sites including the apexes of the square inclusions. Cells of this lattice are supposed to be finite elements. The size of a FE is taken at least three times smaller than the minimum thickness a of the host streak between the inclusions (see Fig. 1). Displacements $\mathbf{u}$ inside a FE are approximated by means of nodal displacements $\mathbf{U} = (U_1, U_2)$, using the two-power interpolation. In this way the discrete problem of minimization of the positively defined quadratic form

$$W(\mathbf{U}) = \mathbf{U}^T \mathbf{W} \mathbf{U} \tag{3}$$

is introduced instead of the continuous analog (2). The components of the matrix $\mathbf{W}$ are expressed via the components of the elastic modulus tensor of the host and inclusions. The minimum of $W(\mathbf{U})$ can be reached on a set of displacements $\mathbf{U}$ of nodes satisfying linear equilibrium equations inside $\Omega^{(n)}$,

$$\mathbf{W}\mathbf{U} = \mathbf{0}, \tag{4}$$

and the appropriate boundary conditions at the outer sides of the composite.

The components $C^{(n)}_{1111}$ and $C^{(n)}_{1212}$ of the effective elastic modulus tensor are computed under periodic boundary conditions along the x_1 axis,

$$\mathbf{U}(0,x_2)=\mathbf{U}(l,x_2), \quad x_2\in(0,l), \tag{5}$$

and the fixed displacements on the bottom and top bars, respectively,

$$\mathbf{U}(x_1,0)=\mathbf{0}, \quad \mathbf{U}(x_1,l)=\mathbf{T}, \quad x_1\in(0,l). \tag{6}$$

The boundary conditions (5) and (6) imply that

$$\varepsilon^{(n)}_{11}=0, \quad \varepsilon^{(n)}_{i2}=T_i/l, \quad \sigma_{i2}=F_i/l \quad (i=1,2), \tag{7}$$

where **F** is a force applied to the top bar of the outer side of the carpet. Equations (1) and (7) lead to the following relationships:

$$C^{(n)}_{1212}=F_1/T_1, \quad C^{(n)}_{1111}=C^{(n)}_{2222}=F_2/T_2. \tag{8}$$

In order to calculate $C^{(n)}_{1122}$ the following boundary conditions have to be set on the vertical and horizontal bars of the carpet, respectively:

$$U_1(0,x_2)=0, \quad U_1(l,x_2)=R_1,$$

$$\sigma_{12}(0,x_2)=\sigma_{12}(l,x_2)=0, \quad x_2\in(0,l), \tag{9}$$

$$U_2(x_1,0)=U_2(x_1,l)=0, \quad \sigma_{12}(x_1,0)=\sigma_{12}(x_1,l)=0,$$

$$x_1\in(0,l), \tag{10}$$

where $\mathbf{R}=(R_1,0)$ is the fixed displacement of the right hand bar.

Equations (3), (9), and (10) along with Eq. (1) imply that

$$\varepsilon^{(n)}_{11}=T_1/l, \quad \varepsilon^{(n)}_{12}=\varepsilon^{(n)}_{22}=0, \quad \sigma^{(n)}_{22}=F_2/l,$$

$$C^{(n)}_{1122}=\sigma^{(n)}_{22}/\varepsilon^{(n)}_{11}=F_2/R_1. \tag{11}$$

In order to calculate the effective elastic moduli of the Sierpinski carpet, it is sufficient to determine the macroscopic force **F** applied to the top layer of the finite elements, as follows from Eqs. (8) and (11). The idea of using the transfer matrix method [4,5] allows one to calculate this force without complete numerical solution of the boundary value problem and, therefore, to use a computer more efficiently. The corresponding numerical algorithms and codes have been elaborated and used to estimate the effective modulus tensor $C^{(n)}_{ijkl}$.

It should be emphasized that direct use of this code for a highly developed fractal (large n) requires a huge number of finite elements and therefore becomes impossible. For this reason, we shall restrict use of the FEM up to the fourth initial generation of the carpet.

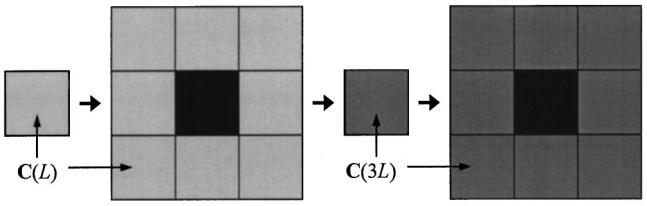

FIG. 2. The scheme of the iterative procedure for the derivation of the effective elastic properties of well-developed Sierpinski-like carpets using a structural cell of first order.

B. Position-space renormalization group technique

In order to study elastic properties of developed fractal composites with a large amount of generations, the position-space renormalization group can be employed. This technique has been used before for discrete spring-based models of isotropic percolation [10]. In order to adapt it for a continuous elastic fractal a set of steps must be carried out. The first one includes FEM-based calculations of the effective moduli of one of the first initial generations of the Sierpinski carpet ($n=1,2,3,4$). This generation will be called here a *structural cell* of the nth order. The procedure determines the mapping

$$\mathbf{f}^{(n)}: \ \mathbf{C}^{(0)}\rightarrow\mathbf{C}^{(n)} \tag{12}$$

of the host elastic modulus $\mathbf{C}^{(0)}=\{C^{(0)}_{ijkl}\}$ to that of the Sierpinski carpet of the nth generation $\mathbf{C}^{(n)}=\{C^{(n)}_{ijkl}\}$. The next step is to use these effective moduli for the renormalized host of the carpet having the same level of generation. Then the procedure is reiterated. After m steps we reach the mnth generation of the carpet (corresponding to $L=3^{nm}$). The scheme of such operations is illustrated in Fig. 2 with $n=1$. Thus, the effective elastic moduli $\mathbf{C}^{(mn)}$ of the mnth generation of the carpet can be estimated using mapping (12) m times over:

$$\mathbf{C}^{(0)} \underbrace{\xrightarrow{\mathbf{f}^{(n)}} \mathbf{C}^{(n)} \xrightarrow{\mathbf{f}^{(n)}} \cdots \xrightarrow{\mathbf{f}^{(n)}}}_{m} \mathbf{C}^{(mn)}. \tag{13}$$

It is evident that the accuracy of the results obtained with the method suggested depends on two factors. The first one is the accuracy of the numerical calculations with the FEM. The error can be diminished by appropriate choice of the finite element size, which is supposed to be done. The second factor is the level n of the structural cell. It assigns the mapping $\mathbf{f}^{(n)}$, used to calculate the elastic modulus of the renormalized host at each step of iteration (13). The influence of the last factor may be explained by the following example. The effective elastic moduli of the carpet of the size $L=3^{nm}$ can be calculated in two ways: (i) the successive applications of m iterations of mapping $\mathbf{f}^{(n)}$ or (ii) the same with mn iterations of mapping $\mathbf{f}^{(1)}$. Each can lead to different results not matching the exact solution. This ambiguity cannot be excluded because of the restrictions on the numerical procedure discussed in the previous subsection. The significance of this factor will be discussed in the next sections.

III. EFFECTIVE ELASTIC PROPERTIES OF THE SIERPINSKI CARPET

A. Fixed-point problem

Because the inclusions considered in this paper have zero or infinite rigidity, the mapping (12) is expressed by a first order homogeneous function for both elastic and superelastic carpets:

$$\mathbf{f}^{(n)}(\lambda \mathbf{C}) = \lambda \mathbf{f}^{(n)}(\mathbf{C}). \tag{14}$$

This property makes it possible to consider just two independent ratios of three elastic moduli of the carpet. We have chosen the effective Poisson ratio ν and the coefficient of anisotropy α,

$$\nu = \frac{C_{1122}}{C_{1111}}, \quad \alpha = \frac{C_{1111} - C_{1122}}{2C_{1212}}, \tag{15}$$

which have a clear physical meaning. The Poisson ratio ν is a measure of the transverse contraction caused by uniaxial tension. The coefficient of anisotropy α is the degree of deviation of the effective elastic moduli of an anisotropic material of square symmetry from those of isotropic materials ($\alpha = 1$ for isotropic media). First order homogeneity of the effective elastic moduli, given by Eq. (14), leads to zero order homogeneity of the ratios defined by Eq. (15). This makes it possible to introduce the transformation

$$\mathbf{r}^{(n)}: \ (\nu^{(0)}, \alpha^{(0)}) \to (\nu^{(n)}, \alpha^{(n)}) \tag{16}$$

which determines the mapping of the Poisson ratio and the coefficient of anisotropy of the host to those of the nth generation of the Sierpinski carpet. The main purpose is to show numerically that successive applications of $\mathbf{r}^{(n)}$ would result in the fixed point $(\overline{\nu}^{(n)}, \overline{\alpha}^{(n)})$. The fixed point corresponds to the effective Poisson ratio and the coefficient of anisotropy of a well-developed Sierpinski carpet produced by many iterations of the structural cell $\Omega^{(n)}$. The fixed point must obey the equation

$$(\overline{\nu}^{(n)}, \overline{\alpha}^{(n)}) = \mathbf{r}^{(n)}(\overline{\nu}^{(n)}, \overline{\alpha}^{(n)}), \tag{17}$$

representing the contraction property of the mapping $\mathbf{r}^{(n)}$. If a solution of this problem exists, it means that all the components of the elastic modulus tensor yield an exact scaling law with a common exponent. Indeed, if the host moduli are taken to be equal to the values provided by Eq. (17), the effective Poisson ratio and the coefficient of anisotropy should be independent of the size of the carpet, i.e.,

$$(\nu^{(0)}, \alpha^{(0)}) = (\nu^{(mn)}, \alpha^{(mn)}) = (\overline{\nu}^{(n)}, \overline{\alpha}^{(n)}). \tag{18}$$

The last equalities can be fulfilled only if the exact scaling law for all the components of the tensor of the elastic moduli holds:

$$C_{ijkl} = C^{(0)}_{ijkl} L^{\beta^{(n)}}. \tag{19}$$

The exponent $\beta^{(n)}$ is equal to $-\tau^{(n)}$ or $s^{(n)}$ depending on whether an elastic or superelastic fractal is considered. The last values can be calculated with the use of one of the components of the mapping $\mathbf{f}^{(n)}$ given by Eq. (12):

$$\beta^{(n)} = \frac{1}{n \ln 3} \ln\left[f^{(n)}_{1111}\left(1, \overline{\nu}^{(n)}, \frac{1-\overline{\nu}^{(n)}}{2\overline{\alpha}^{(n)}}\right)\right]. \tag{20}$$

In the general case, the contractive property of the reduced mapping $\mathbf{r}^{(n)}$ will provide a gradual convergence to the fixed point of the ratios of the effective elastic moduli:

$$(\nu^{(mn)}, \alpha^{(mn)}) \to (\overline{\nu}^{(n)}, \overline{\alpha}^{(n)}), \quad m \to \infty, \tag{21}$$

and the scaling law (19) for the moduli will occur asymptotically (see the next subsection).

The convergence (21) has been numerically verified by means of calculation of the flow diagrams in the (ν, α) plane for both elastic and superelastic Sierpinski carpets. The results are shown in Figs. 3(a) and 3(b), respectively. The solid lines in the diagrams represent the trajectories of the iterative procedures with a structural cell of order $n = 2$. The starting positions of the trajectories are given by the parameters of

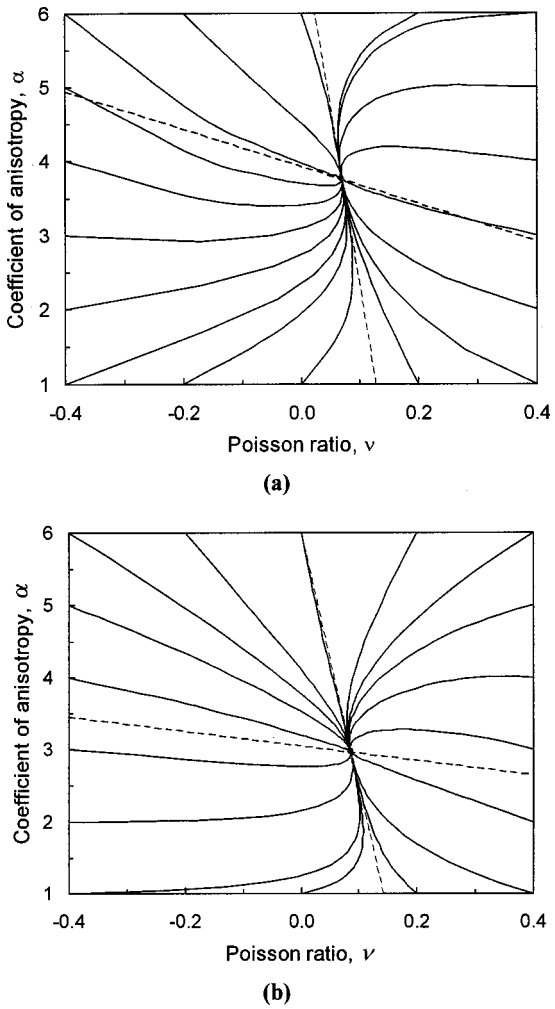

FIG. 3. The flow diagrams calculated by the iterative mapping (13) with a structural cell of second order for the (a) elastic and (b) superelastic Sierpinski carpets. The dotted lines are directed along eigenvectors of the linearized mapping (23).

TABLE I. Effective Poisson ratio $\overline{\nu}^{(n)}$, coefficient of anisotropy $\overline{\alpha}^{(n)}$, and scaling exponents $\tau^{(n)}$ and $s^{(n)}$ at the fixed points of the elastic and superelastic Sierpinski carpets generated by a structural cell of the order of n.

n	1	2	3	4	∞
			Elastic Sierpinski carpet		
$\overline{\nu}^{(n)}$	0.075	0.069	0.066	0.066	0.065
$\overline{\alpha}^{(n)}$	3.02	3.77	4.23	4.33	4.43
$\tau^{(n)}$	0.298	0.296	0.291	0.284	0.284
			Superelastic Sierpinski carpet		
$\overline{\nu}^{(n)}$	0.103	0.085	0.075	0.064	0.063
$\overline{\alpha}^{(n)}$	2.42	2.97	3.33	3.70	3.74
$s^{(n)}$	0.186	0.170	0.168	0.169	0.168

the host. It is clearly seen that all the trajectories in each diagram converge to a common fixed point without regard to their starting positions. This important result brings us to the conclusion that *effective elastic properties of the well-developed Sierpinski carpet are independent of the elastic properties of the host*. The difference between the fixed points of the elastic and superelastic carpets depends exclusively on the values of the elastic moduli of the inclusions. The same conclusions were obtained for some other structural cells considered. The data are summarized in Table I for $n=1$, 2, 3, and 4 together with the limits corresponding to $n\to\infty$ for the elastic and superelastic Sierpinski carpets.

Consider briefly the evidence of the contraction of mapping (16). Geometrically the contraction signifies a reduction in distance between two arbitrary points (ν_1,α_1) and (ν_2,α_2) in the flow diagram. This property can be expressed by the following inequality:

$$\|\mathbf{r}^{(n)}(\nu_2,\alpha_2)-\mathbf{r}^{(n)}(\nu_1,\alpha_1)\|\leqslant\delta\|(\nu_2,\alpha_2)-(\nu_1,\alpha_1)\| \tag{22}$$

with arbitrary positive δ less than 1. Direct proof of the relationship (22) can be given in the near vicinity of a fixed point. In this case all terms except the linear ones can be neglected in the Taylor expansion of the mapping $\mathbf{r}^{(n)}$ and Eq. (17) may be rewritten as follows:

$$\mathbf{r}^{(n)}(\nu,\alpha)-(\overline{\nu}^{(n)},\overline{\alpha}^{(n)})\approx(\nu-\overline{\nu}^{(n)},\alpha-\overline{\alpha}^{(n)})\mathbf{R}^{(n)}. \tag{23}$$

The matrices $\mathbf{R}^{(n)}$ together with their eigenvalues $\lambda_i^{(n)}$ and eigenvectors $\mathbf{e}_i^{(n)}$ can be found numerically in the framework of the FEM described above. The results are represented in Table II for $n=2$ for elastic and superelastic composites.

It is seen that the eigenvalues satisfy the inequalities $|\lambda_i^{(2)}|<1$, $i=1,2$, which proves that mapping (16) is a contractive one. The directions of the eigenvectors are shown by dotted lines in Fig. 3. The tangential line corresponds to the largest eigenvalue. The convergence of the flow diagrams to the fixed point is evident.

The results obtained are slightly dependent on level n. The limit $n\to\infty$ is obviously important to know. An attempt to estimate it was made by a two-power polynomial approximation of the data corresponding to finite values of n with respect to the variable $\varepsilon=1/n$. The results are represented in the last column of Table I. They are close to the estimates corresponding to $n=4$, which provides a reasonable accuracy of the parameters at the fixed point.

TABLE II. Linearized mapping $\mathbf{R}^{(2)}$ for the elastic and superelastic Sierpinski carpets.

$\mathbf{R}^{(2)}$	Eigenvalues of $\mathbf{R}^{(2)}$	Eigenvectors $\mathbf{R}^{(2)}$
	Elastic Sierpinski carpet	
$\begin{pmatrix}0.51 & -0.005\\ 0.64 & 0.77\end{pmatrix}$	0.76; 0.52	(−0.02 1); (0.37 −0.93)
	Superelastic Sierpinski carpet	
$\begin{pmatrix}0.79 & -0.003\\ 0.21 & 0.91\end{pmatrix}$	0.9; 0.8	(−0.03 1); (0.46 −0.89)

B. Comparison of elastic properties of the initial and developed generations of the Sierpinski carpet

As was mentioned, the finite-element method can be applied in practice only for a few initial generations of the continuous fractal. The results of these calculations for four generations of the elastic and superelastic Sierpinski carpet are represented in Fig. 4 as logarithmic relationships of three effective elastic moduli C_{1111}, C_{1122}, and C_{1212} with dimensionless size L of the system. Two values of the Poisson ratio for the isotropic host, $\nu^{(0)}=0.2$ and 0.8, were considered. It is seen that in this range of the generations approximate linear dependencies of $\log_{10}(C)$ vs $\log_{10}(L)$ occur only at $\nu^{(0)}=0.2$ for the elastic carpet [see Fig. 4(a)]. The slopes of these lines are different for different components of the effective elastic modulus tensor. This observation confirms the predictions of Refs. [8,9]. However, the curves are nonlinear, especially with $\nu^{(0)}=0.8$ [see Fig. 4(b)]. This indicates that generally the elastic moduli of the fractal composite do not obey scaling behavior at a small dimensionless size of the system, and study of the developed generations of the Sierpinski carpet becomes essential.

The behavior of $\log_{10}(C)$ versus $\log_{10}(L)$ in a large range of L was studied with the PSRG approach using a structural cell of the order of $n=3$. The results are plotted in Fig. 5 for the example of an elastic (porous) Sierpinski carpet. It is clearly seen that the curves approach the same slope asymptotically giving a common scaling exponent for all components of the effective elastic modulus tensor (see Table I). Moreover, the inequalities $C_{1111}>C_{1212}>C_{1122}$ occur at a reasonably large dimensionless size of the carpet for each value of the host Poisson ratio considered. It can be shown that these inequalities hold for an isotropic matrix if $\nu^{(0)}$ is less than $\frac{1}{3}$. So the plots for $\nu^{(0)}=0.2$ retain this order at arbitrary L and look linear within the whole range of L [see Fig. 5(a)]. However, a departure from the linear behavior at small L becomes evident for higher Poisson ratios of the host, say, $\nu^{(0)}=0.8$. In this case the curves corresponding to C_{1212} and C_{1122} intersect at $\log_{10}(L)\approx 5$ [see Fig. 5(b)].

The change in the slopes of the curves may be conveniently illustrated by the dependence of the logarithmic de-

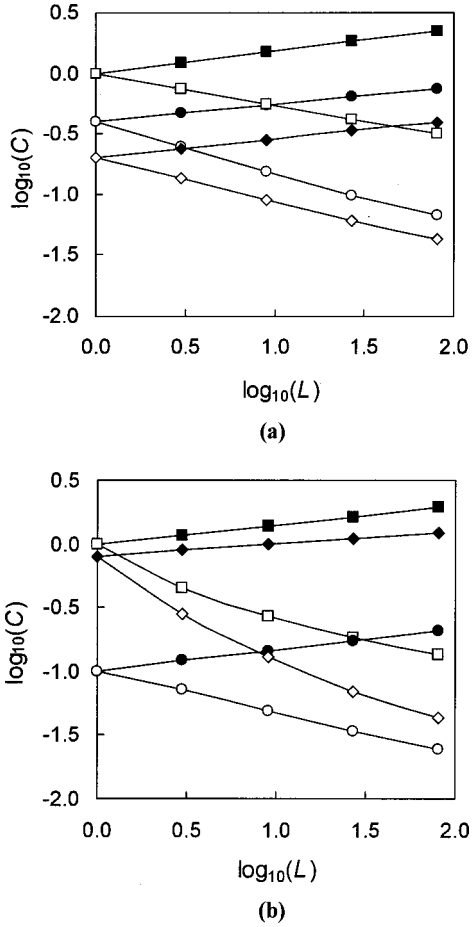

FIG. 4. The dependence of the effective elastic moduli, calculated by direct application of the FEM, on the dimensionless size L of the Sierpinski carpet. $\nu^{(0)}=$ (a) 0.2; (b) 0.8. The moduli of the elastic composite are indicated by the empty squares (C_{1111}), diamonds (C_{1122}), and circles (C_{1212}). The filled markers mark the corresponding moduli of the superelastic carpet.

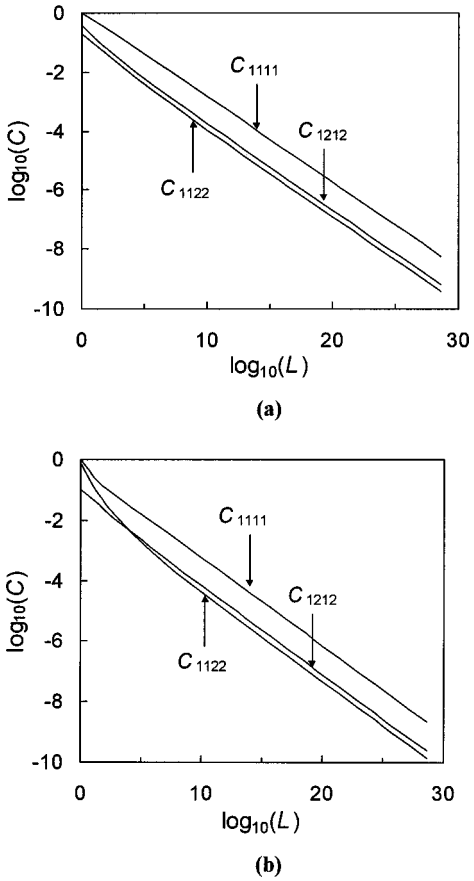

FIG. 5. The dependence of the effective elastic moduli calculated by means of the PSRG technique with a structural cell of order 3 on the dimensionless size L of the elastic Sierpinski carpet with isotropic host: $\nu^{(0)}=$ (a) 0.2 and (b) 0.8.

rivatives of the effective elastic moduli on $\log_{10}(L)$. It is shown in Fig. 6 with the example of $d\log_{10}(C_{1122})/d\log_{10}(L)$ for an elastic carpet with $\nu^{(0)}=0.2$. We can see that even in this partial case the evolution of the slope is rather complicated in a wide range of L. It is obvious that the results of the calculations might be dependent on the order of the structural cell used in the renormalization procedure. Indeed, the distinction between the data obtained with the PSRG for different structural cells of order $n=1$ and 3 is visible in Fig. 6. Nevertheless, these results are qualitatively identical and almost coincide.

Concluding this part, it is instructive to give more examples demonstrating convergence to the scaling laws and the fixed points of various effective constants of the carpet with different hosts. The data were obtained by PSRG for a structural cell of the order of $n=3$.

The behavior of the logarithmic derivatives of the effective elastic moduli with respect to $\log_{10}(L)$ for the superelastic Sierpinski carpet at $\nu^{(0)}=0.4$ is shown in Fig. 7. It can be seen that all the elastic moduli converge to the common scaling at large dimensionless size of the carpet ($L\geqslant 3^{30}$). The order of L showing truly elastic scaling for the superelastic carpet coincides with that for the porous carpet (compare with Fig. 6). The asymptote of the curves has a slope corresponding to the scaling exponent given in Table I.

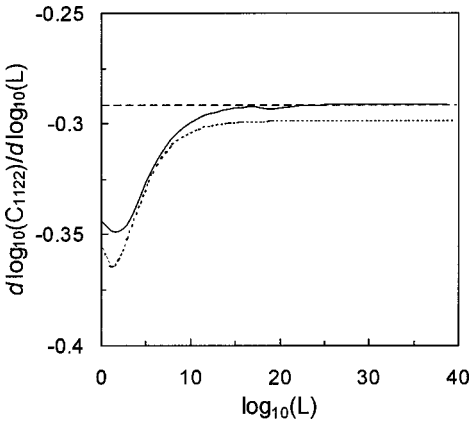

FIG. 6. The dependence of logarithmic derivative $d\log_{10}(C_{1122})/d\log_{10}(L)$ on the dimensionless size L of the elastic Sierpinski carpet with an isotropic host ($\nu^{(0)}=0.2$), calculated by means of the PSRG technique for two structural cells corresponding to $n=1$ (dotted line) and 3 (solid line).

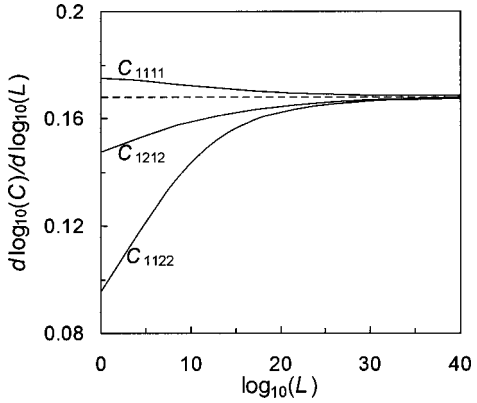

FIG. 7. The dependencies of the logarithmic derivative of three independent components of the effective elastic modulus tensor on the dimensionless size L of the superelastic Sierpinski carpet with isotropic host ($\nu^{(0)}=0.4$).

Figure 8(a) demonstrates the behavior of the effective Poisson ratio of the elastic Sierpinski carpet as a function of its dimensionless size in the curious case of negative host Poisson ratio $\nu^{(0)}=-0.2$. It can be seen that the effective

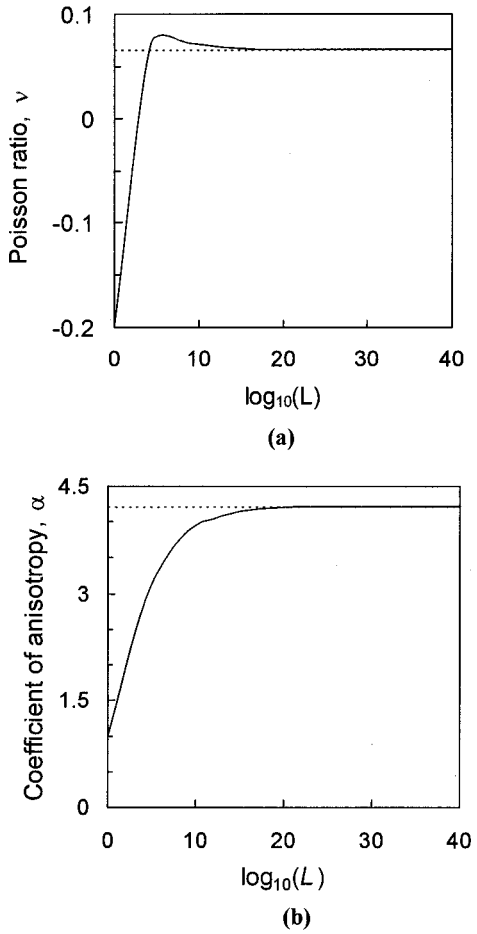

FIG. 8. The convergence to asymptotic values (fixed points) of (a) the effective Poisson ratio and (b) the coefficient of anisotropy of the elastic Sierpinski carpet with isotropic host at negative Poisson ratio $\nu^{(0)}=-0.2$.

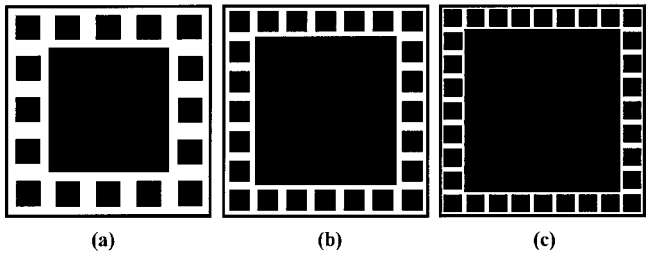

FIG. 9. The second generation of Sierpinski-like carpets with different fractal dimensions. (a) $D=1.7227$ ($k=5$), (b) $D=1.6332$ ($k=7$), and (c) $D=1.5773$ ($k=9$).

value of this ratio for the developed carpet leads to the universal positive value $\overline{\nu}^{(\infty)}=0.065$ found for other hosts. The same tendency takes place for the superelastic carpet as well (see Table I). The convergence of the effective coefficient of anisotropy α to a fixed value is illustrated in Fig. 8(b) for the elastic fractal. One of the remarkable properties of this constant is that it noticeably exceeds unity for each elastic and superelastic carpet. This means that the composites under consideration are essentially anisotropic.

IV. ELASTIC PROPERTIES AND FRACTAL DIMENSIONS OF SIERPINSKI-LIKE CARPETS

In the previous sections we have discussed the elastic properties of the classical Sierpinski carpet with a fixed fractal dimension. Qualitatively, it is evident that the results obtained (the fixed-point positions, scaling exponents, etc.) should change with fractal dimension. We are going to discuss this problem in this section.

The relationship between elastic exponents and the fractal dimension of the continuous matrix composites is unknown. To clarify this point in the framework of the square symmetry inherent in the Sierpinski carpet we consider some of its generalizations. The set of these structures will be called Sierpinski-like carpets. These objects are constructed in the following way. Dividing the outer side by integer number k and then removing a central part with a side of size proportional to $k-2$ we obtain the first generations of the carpets. The next step comprises a division of the remaining $4k-4$ square elements in a similar way. Examples of the second generations of such fractals for $k=5$, 7, and 9 are shown in Fig. 9. Their fractal dimensions are given by the following relationship:

$$D=\log_{10}(4k-4)/\log_{10}(k). \tag{24}$$

In the case of the Sierpinski carpet $k=3$ which provides the known value $D=1.893$. Fractal dimensions of the Sierpinski-like structures at $k=5$, 7, and 9 are equal to 1.723, 1.633, and 1.577, respectively. These fractals are characterized by the same square symmetry as the Sierpinski carpet and their elastic properties can be described by the same set of parameters considered in the above sections: three elastic moduli, the Poisson ratio, and the anisotropy coefficient. Calculating these values for the carpets intro-

TABLE III. Effective Poisson ratio $\overline{\nu}^{(n)}$, coefficient of anisotropy $\overline{\alpha}^{(n)}$, and scaling exponents $\tau^{(n)}$ and $s^{(n)}$ at the fixed points of the elastic and superelastic Sierpinski-like carpets of different fractal dimension D generated by structural cells of the order of $n=1$ and 2.

k	D	$\overline{\nu}^{(n)}$	$\overline{\alpha}^{(n)}$	$\tau^{(n)}$
		Elastic Sierpinski-like carpet		
		$n=1$		
5	1.7227	0.009 89	13.625	0.550 70
7	1.6332	0.002 19	44.271	0.637 16
9	1.5773	0.000 70	107.69	0.681 39
		$n=2$		
5	1.7227	0.005 33	56.164	0.553 61
7	1.6332	0.000 52	626.06	0.639 56
9	1.5773	0.000 15	2506.0	0.673 07
		Superelastic Sierpinski-like carpet		
		$n=1$		
5	1.7227	0.026 92	4.8931	0.438 90
7	1.6332	0.013 03	7.1097	0.554 55
9	1.5773	0.007 72	9.2284	0.618 73
		$n=2$		
5	1.7227	0.017 49	6.0997	0.427 38
7	1.6332	0.006 96	8.3994	0.546 44
9	1.5773	0.002 28	11.3180	0.618 91

duced, we can derive the change in the scaling exponents and fixed points with changing fractal dimension.

The strategy of the calculation of the elastic properties for the Sierpinski-like structures is similar to that described in the previous sections for the classical Sierpinski carpet. The final results of the renormalization group analysis are summarized in Table III. We restricted ourselves here to two sets of data with structural cells of the order of 1 and 2. Using these results together with those obtained for the Sierpinski carpet, we can draw the dependencies of different elastic characteristics (effective Poisson ratio, effective coefficient of anisotropy, and scaling exponents) on the fractal dimension. They are represented in Fig. 10 calculated by means of the PSRG technique with corresponding structural cells of order $n=1$. The black circles represent data for superelastic fractals (composites filled by rigid particles) while the empty circles belong to the elastic ones (porous carpets). Notice that the same kind of behavior was observed for $n=2$ excluding larger values of the coefficients of anisotropy.

The following remarkable properties of the structures considered should be emphasized. There is a decrease of the effective Poisson ratio and an increase of the coefficient of anisotropy with increase of the order n of the structural cells and a diminution of the fractal dimension D of the carpets [see Tables I and III, Figs. 10(a) and 10(b)]. It was observed that these regularities are more marked in the case of porous composites than that of superelastic ones. Quantitative analysis of the results shows that these properties of Sierpinski-like carpets are realized due to the enormous growth of C_{1111} with increasing L or n in comparison with the values of other components of the effective modulus tensor. In other words,

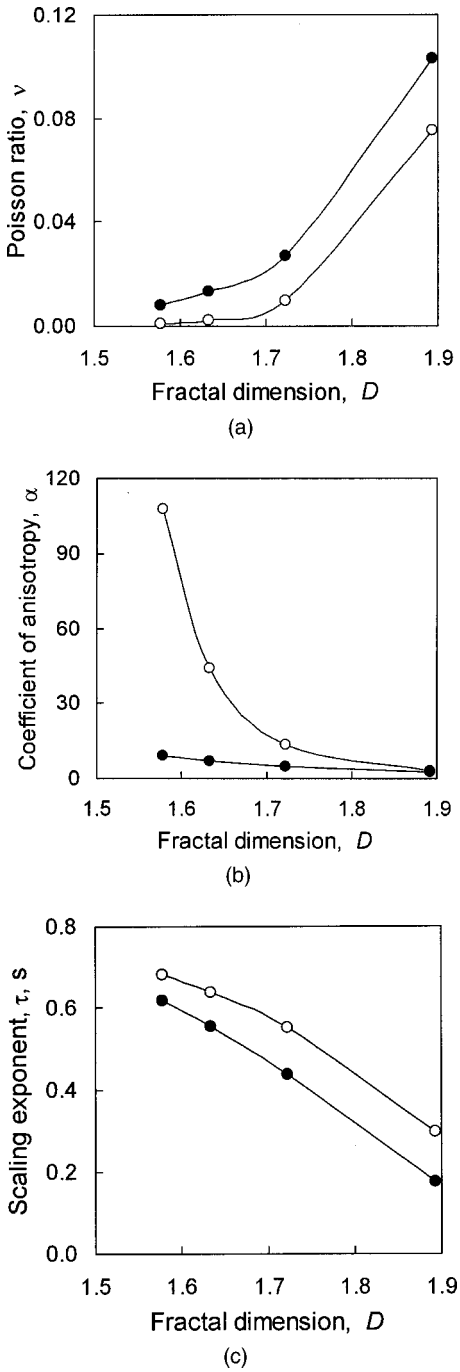

FIG. 10. The dependence on the fractal dimension (a) for the effective Poisson ratios, (b) for the coefficients of anisotropy, and (c) for the scaling exponents of well-developed Sierpinski-like carpets. The filled and empty circles correspond to the elastic and superelastic carpets, respectively. Calculations were made by means of the PSRG technique with corresponding structural cells of first order.

the development of a fractal structure of the composites brings their elastic response close to the behavior of unidimensional elastic materials.

The nature of this phenomenon may be understood if we take into account a decrease of the cross sections of the ligaments of the host between inclusions with increasing number

of generations. A complex distribution of the strain and stress fields inside the streaks can lead to the results discussed. This outcome, seen in Tables I and III, is confirmed by the sensitivity of the data obtained to the values of n and D and the type of inclusion. Actually, the increase of order n of the structural cell makes calculations of stress and strain in the host more precise. It shifts the Poisson ratio and the coefficient of anisotropy toward lower and higher values, respectively. The decrease of fractal dimension would just emphasize this tendency because it leads to a decrease of the host fraction and thus makes the streaks between the inclusions thinner. As to the type of inclusion, the stress-strain states of the host are different for porous and filled materials. The data obtained show that the porous fractals reveal themselves as unidimensional elastic media to a greater extent than the composites filled with rigid inclusions.

It is shown in Fig. 10(c) that scaling exponents of elastic and superelastic Sierpinski-like carpets decrease with increase of the fractal dimension. This sort of behavior of the exponents may be predicted in general. Actually, if the fractal dimension is getting closer to the original space dimension, the dependence of the effective elastic moduli on the dimensionless size of the fractal should be less pronounced. In the limiting case of $d=D$ there is no dependence of L at all and the exponents should equal zero.

As in the case of the classical Sierpinski carpet, the effective elastic properties of the developed Sierpinski-like structures are independent of the host. This remarkable property is illustrated in Fig. 11 by flow diagrams calculated with a structural cell of the order of $n=1$ for both elastic and superelastic carpets with fractal dimension $D=1.6332$. The fixed-point analysis, produced in the same way as in Sec. III A, confirms this conclusion. The dotted lines in these plots show directions of eigenvectors, crossing the fixed points. It suggests that only fractal dimension and rigidity of inclusions determine the effective elastic properties of composites with developed structure.

V. CONCLUSIONS

The effective elastic properties of 2D continuous elastic (porous) and superelastic (filled by rigid particles) fractal composites with the structures of Sierpinski-like carpets have been studied. A combined technique based on the finite element method and the position-space renormalization group procedure was developed toward this end. A convergence to a fixed point was studied by a flow diagram in the plane of the current Poisson ratios and anisotropy coefficients. The fixed points were found to exist for both elastic and superelastic carpets. But the convergence becomes apparent after more than 30 steps of partitions. It provides a true elastic self-similarity just for carpets with a well-developed structure. This means that effective elastic moduli do not obey the scaling behavior in the initial generations of the carpets (except for the host moduli, equal to those of the fixed point).

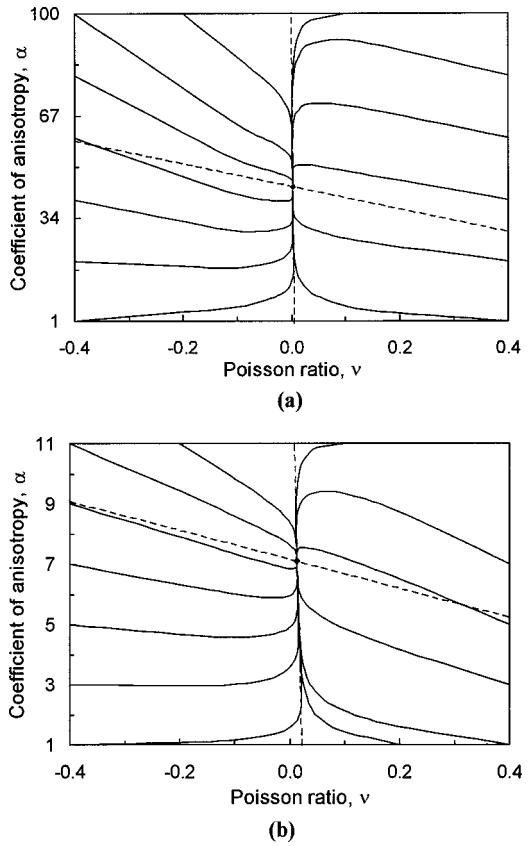

FIG. 11. Flow diagrams of the (a) elastic and (b) superelastic Sierpinski-like carpets of fractal dimension $D=1.6332$ calculated with a structural cell of first order. The dotted lines correspond to eigenvectors of the linearized mapping (23).

A common exponent for all the components of the elastic modulus tensor characterizes elastic scaling. Different exponents describe the scaling behavior of elastic and superelastic carpets. The fixed points were found to be independent of the elastic properties of the host. So we may conclude that the fractal dimension and the type of inclusion are the most relevant parameters governing the elastic scaling of continuous composites.

Increase of the dimensionless size L and of the order n of the structural cell and decrease of the fractal dimension D of the composites lead to diminution of the effective Poisson ratio and increase of the coefficient of anisotropy. This makes the elastic behavior of the developed continuous composites close to that of unidimensional materials. The scaling exponents increase with decrease of the fractal dimension in both cases of elastic and superelastic Sierpinski-like carpets.

ACKNOWLEDGMENT

This work was partially supported by the Russian Foundation for Basic Research (Grant Nos. 00-03-33169 and 01-03-32237).

[1] S. Feng and P. N. Sen, Phys. Rev. Lett. **52**, 216 (1984).
[2] Y. Kantor and I. Webman, Phys. Rev. Lett. **52**, 1891 (1984).
[3] D. J. Bergman and Y. Kantor, Phys. Rev. Lett. **53**, 511 (1984).
[4] E. Duering and D. J. Bergman, Phys. Rev. B **37**, 9460 (1988).
[5] E. Duering and D. J. Bergman, Physica A **157**, 561 (1989).
[6] S. Arbabi and M. Sahimi, Phys. Rev. B **47**, 695 (1993); **47**, 703 (1993).
[7] P. Meakin, in *Random Fluctuations and Pattern Growth: Experiments and Models*, edited by H. E. Stanley and N. Ostrowsky, Vol. 157 of *NATO Advanced Study Institute, Series E: Applied Sciences* (Plenum, New York), p. 174.
[8] P. Sheng and R. Tao, Phys. Rev. B **31**, 6131 (1985).
[9] S. A. Patlazhan, in *Mechanics of Polymer Composites*, Proceedings of the Third International Symposium MPC'91, edited by R. A. Bareš (Institute of Theoretical and Applied Mathematics of the Czechoslovak Academy of Science, Prague, 1991), p. 221.
[10] S. Feng and M. Sahimi, Phys. Rev. B **31**, 1671 (1985).